

Supplementary material

Dicyemida and Orthonectida: Two stories of body plan simplification

Oleg A. Zverkov¹, Kirill V. Mikhailov^{1,2}, Sergey V. Isaev^{1,3}, Leonid Y. Rusin^{1,4}, Olga V. Popova², Maria D. Logacheva^{1,2,5}, Alexey A. Penin^{1,4}, Leonid L. Moroz⁶, Yuri V. Panchin^{1,2}, Vassily A. Lyubetsky¹, and Vladimir V. Aleoshin^{1,2*}

¹Institute for Information Transmission Problems, Russian Academy of Sciences, Moscow, 127051, Russian Federation,

²Belozersky Institute for Physico-Chemical Biology, Lomonosov Moscow State University, Moscow, Russian Federation,

³Faculty of Bioengineering and Bioinformatics, Lomonosov Moscow State University, Moscow, Russian Federation,

⁴Faculty of Biology, Lomonosov Moscow State University, Moscow, Russian Federation,

⁵Skolkovo Institute of Science and Technology, Moscow, Russian Federation,

⁶Department of Neuroscience and McKnight Brain Institute, University of Florida, Gainesville, 32611, USA

Table 1 (for page 17). NCBI Sequence Read Archive accessions of transcriptome libraries used in the phylogenetic analysis

Taxonomic group	Species	Experiment ID	Run ID(s)
Acanthocephala	<i>Echinorhynchus gadi</i>	SRX1121912	SRR2131254
Annelida (Errantia)	<i>Glycera tridactyla</i>	SRX516622	SRR1237833,70
	<i>Marpysa bellii</i>	SRX515220	SRR1232833
	<i>Myzostoma cirriferum</i>	SRX516623	SRR1237872
Annelida (Protodrilidae)	<i>Megadrilus</i> sp.	SRX1026327	SRR2020581
	<i>Protodriloides chaetifer</i>	SRX1023293	SRR2016233
	<i>Protodriloides symbioticus</i>	SRX1116278	SRR2124791,92
Annelida (early branches)	<i>Protodrilus adhaerens</i>	SRX1022008	SRR2014684
	<i>Chaetopterus variopedatus</i>	SRX512002	SRR1219647
	<i>Magelona berkeleyi</i>	SRX522872	SRR1257638,39
Brachiopoda	<i>Owenia fusiformis</i>	SRX512807	SRR1222288
	<i>Spiochaetopterus</i> sp.	SRX513557	SRR1224605
	<i>Terebratalia transversa</i>	SRX1015908	SRR2005824
Bryozoa	<i>Membranipora membranacea</i>	SRX1121923	SRR2131259
Dicyemida	<i>Dicyema</i> sp.	SRX265465	SRR827581
Gastrotricha	<i>Diuronotus aspetos</i>	SRX1121926	SRR2131262
	<i>Mesodasys laticaudatus</i>	SRX872416	SRR1797883
Gnathostomulida	<i>Austrognathia</i> sp.	SRX997150	SRR1976176
Kamptozoa	<i>Loxosoma pectinaricola</i>	SRX731476	SRR1611559
	<i>Symbion americanus</i>	SRX1122263	SRR2131690
Micrognathozoa	<i>Limnognathia maerski</i>	SRX1121929	SRR2131287
Mollusca	<i>Chiton olivaceus</i>	SRX205322	SRR618506
Nemertea	<i>Nipponnemertes</i> sp.	SRX647389	SRR1508368
Phoronida	<i>Phoronis australis</i>	SRX1025550	SRR2018856
Platyhelminthes (Catenulida)	<i>Catenula lemnae</i>	SRX871445	SRR1796434
	<i>Stenostomum leucops</i>	SRX951992	SRR1910423
	<i>Stenostomum sthenum</i>	SRX872404	SRR1801788
Platyhelminthes (Trepaxonemata)	<i>Bothrioplana semperi</i>	SRX980750	SRR1955240
	<i>Leptoplana tremellaris</i>	SRX872321	SRR1797726
	<i>Nematoplana coelogynoporoidea</i>	SRX872398	SRR1797817
Rotifera	<i>Lepadella patella</i>	SRX997434	SRR1976570
Sipuncula	<i>Phascolosoma perlucens</i>	SRX755855	SRR1646442

Supplementary Figure S1 (for page 4). Distribution of circular contig lengths in various assemblies. Discrete length distribution is observed in assemblies by SPAdes (based on De Bruijn graphs, k -mer size 55 or 77 bases), as well as Newbler (not based on De Bruijn graphs).

Supplementary Figure S2 (for page 5). Predicted secondary structures of putative mitochondrial tRNAs of *Dicyema* sp. Co-locating genes and paralogs are outlined (solid and dashed, respectively).

Supplementary Figure S3 (for page 13). Bayesian tree of the Spiralia/Lophotrochozoa with inclusion of the Mesozoa. By supplementing **Figure 10**, it depicts the consensus of the three chains that passed the AU-test, while **Figure 10** shows the all four-chains consensus ($maxdiff=1.0$).

Supplementary Figure S4 (for page 13). Maximum likelihood reconstruction with RAxML. The tree was obtained under the PROTCATGTR model; support values are based on 150 rapid bootstrap replicates. Values of 100% are not shown, and corresponding nodes are marked with black dots. Chimeric operational taxonomic units include names of merged species signed with an asterisk.

Supplementary Figure S5 (for page 13). Maximum likelihood reconstruction with IQ-TREE. The inference was performed under the LG+C60+F+G4 model; node support was evaluated with ultrafast bootstrap approximation (1000 replicates). Nodes with 100% support marked with black dots.

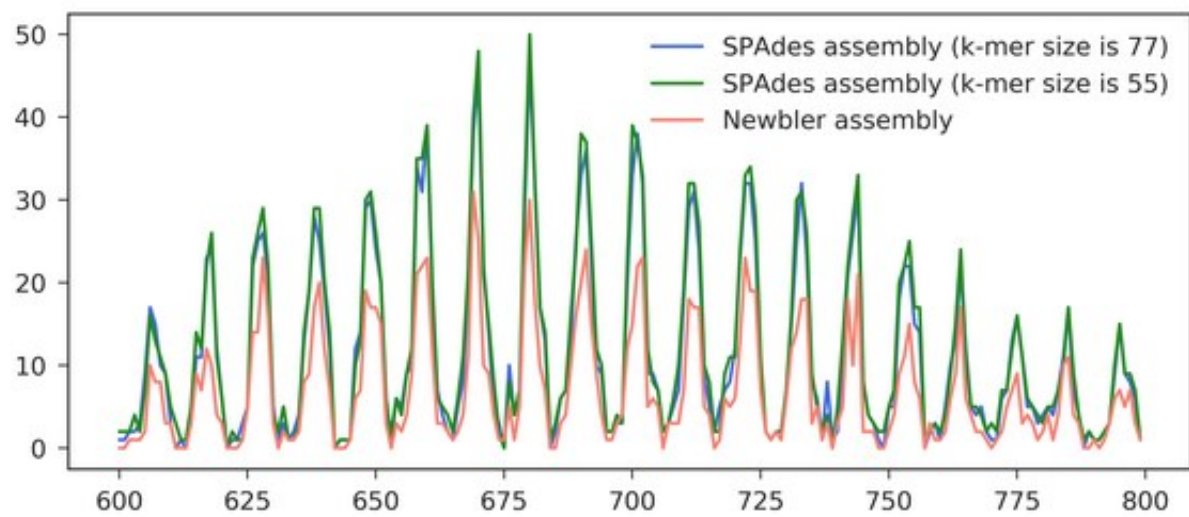
Supplementary Figure S6 (for page 14). Bayesian inference with the dataset excluding the annelid *Myzostoma cirriferum*. PhyloBayes was run with four chains under the CAT+GTR+ Γ 4 model. The consensus tree was constructed after 15,000 cycles with 50% burn-in ($maxdiff=1.0$). Only posterior probability values below 1.0 are shown.

Supplementary Figure S7 (for page 14). Bayesian tree with the exclusion of two dicyemids and the annelid *Myzostoma cirriferum*. PhyloBayes was run with four chains under the CAT+GTR+ Γ 4 model. The consensus tree was constructed after 5,000 cycles with 50% burn-in ($maxdiff=1.0$). Only posterior probability values below 1.0 are shown.

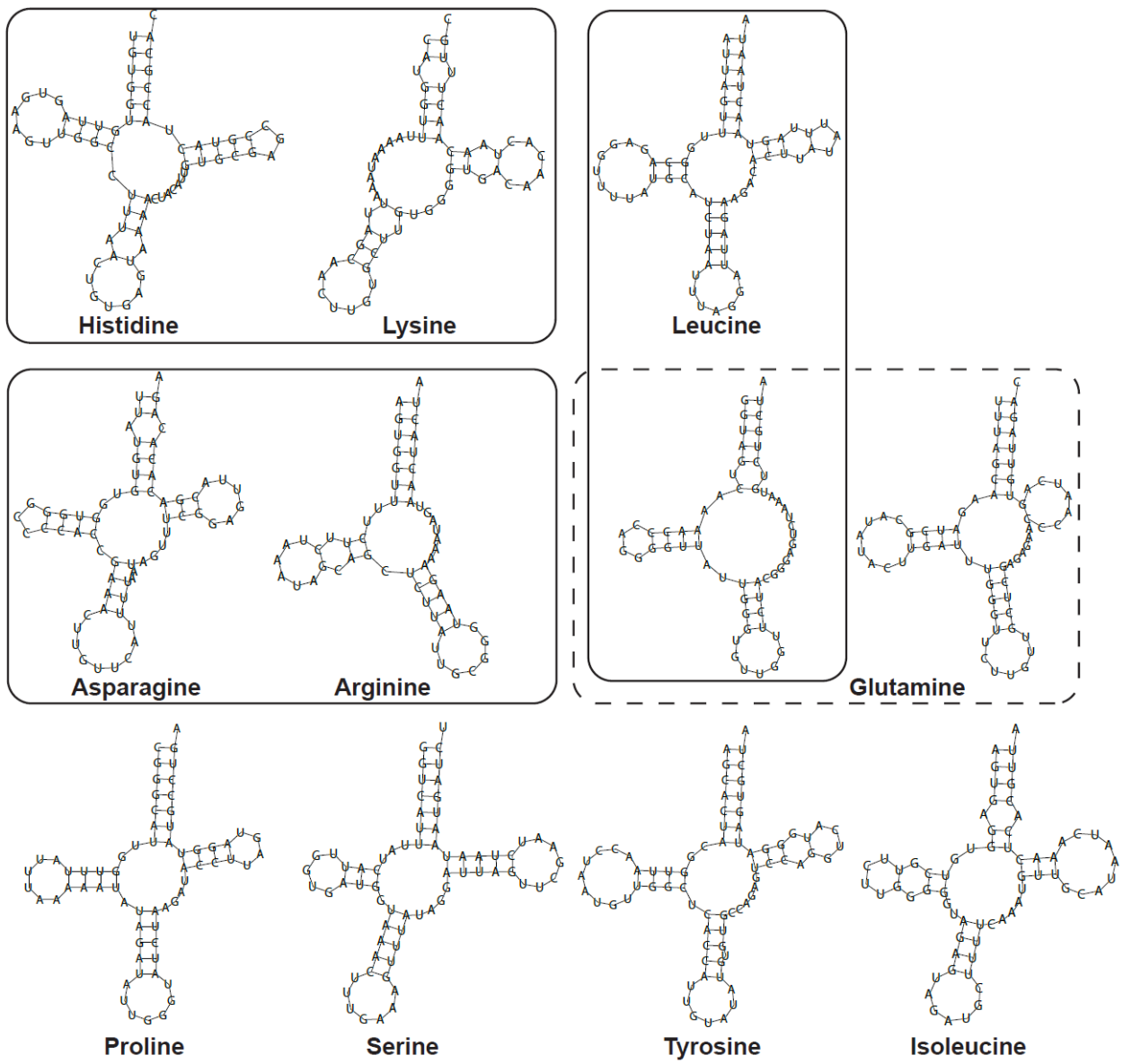
Supplementary Figure S8 (for page 14). Bayesian tree with the exclusion of the orthonectid *Intoschia linei* and the annelid *Myzostoma cirriferum*. PhyloBayes was run with four chains under the CAT+GTR+ Γ 4 model. The consensus tree was constructed after 5,000 cycles with 50% burn-in ($maxdiff=1.0$). Only posterior probability values below 1.0 are shown.

Supplementary Figure S9 (for page 14). Bayesian inference with the 35K-site dataset excluding protein alignments with high compositional heterogeneity. The inference was carried out under the CAT+GTR+ Γ 4 model, and the tree was generated after 50,000 cycles with 50% burn-in ($maxdiff=0.95$).

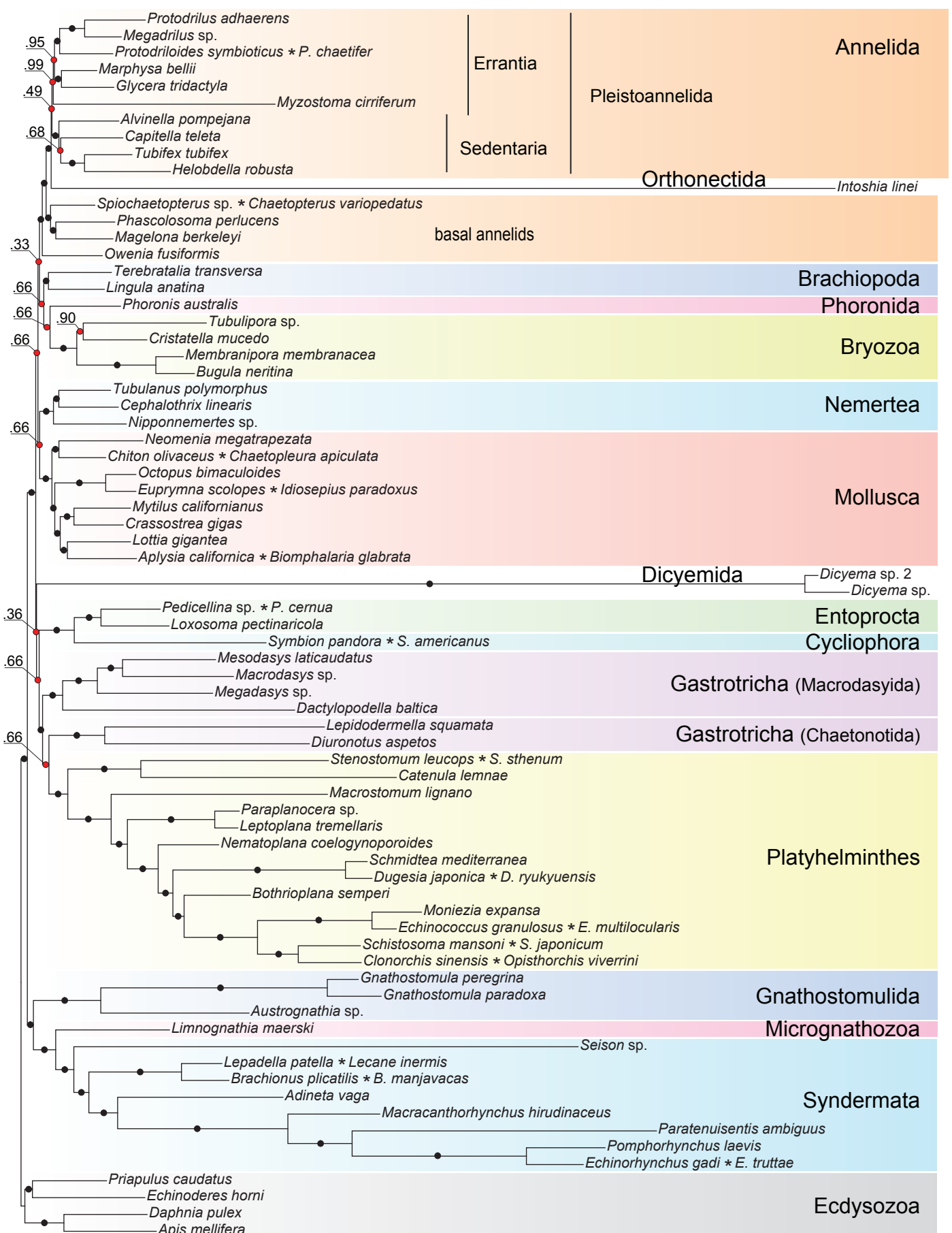
Supplementary Figure S10 (for page 14). Bayesian inference with the Dayhoff-recoded alignment. The inference was carried out under the CAT+GTR+ Γ 4 model; the tree was generated after 30,000 cycles with 50% burn-in ($maxdiff=0.17$).



Supplementary Figure S1 (for page 4). Distribution of circular contig lengths in various assemblies. Discrete length distribution is observed in assemblies by SPAdes (based on De Bruijn graphs, k -mer size 55 or 77 bases), as well as Newbler (not based on De Bruijn graphs).

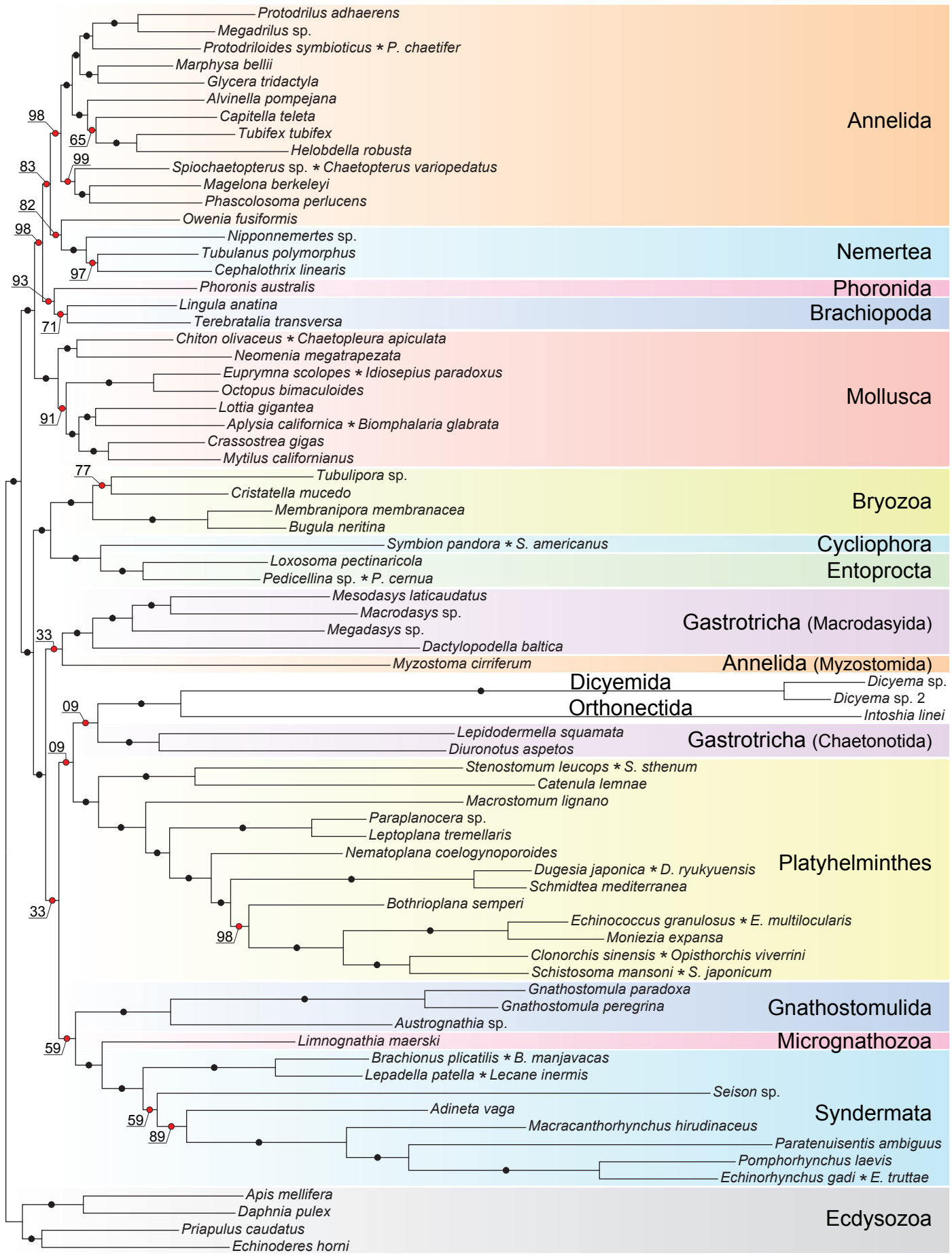


Supplementary Figure S2 (for page 5). Predicted secondary structures of putative mitochondrial tRNAs of *Dicyema* sp. Co-locating genes and paralogs are outlined (solid and dashed, respectively).

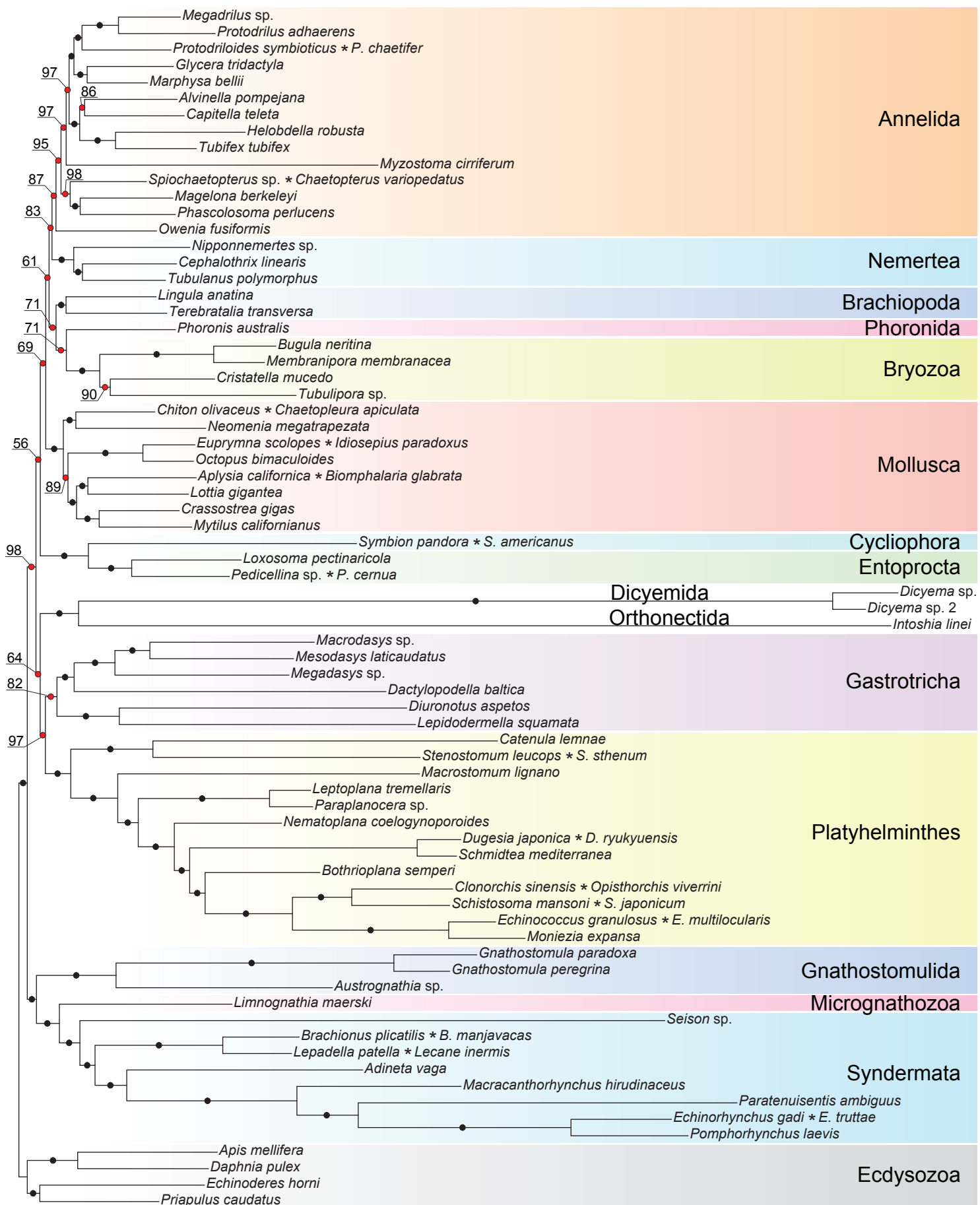


Supplementary Figure S3 (for page 13). Bayesian tree of the Spiralia/Lophotrochozoa with inclusion of the Mesozoa. By supplementing **Figure 10**, it depicts the consensus of the three chains that passed the AU-test, while **Figure 10** shows the all four-chains consensus (*maxdiff*=1.0).

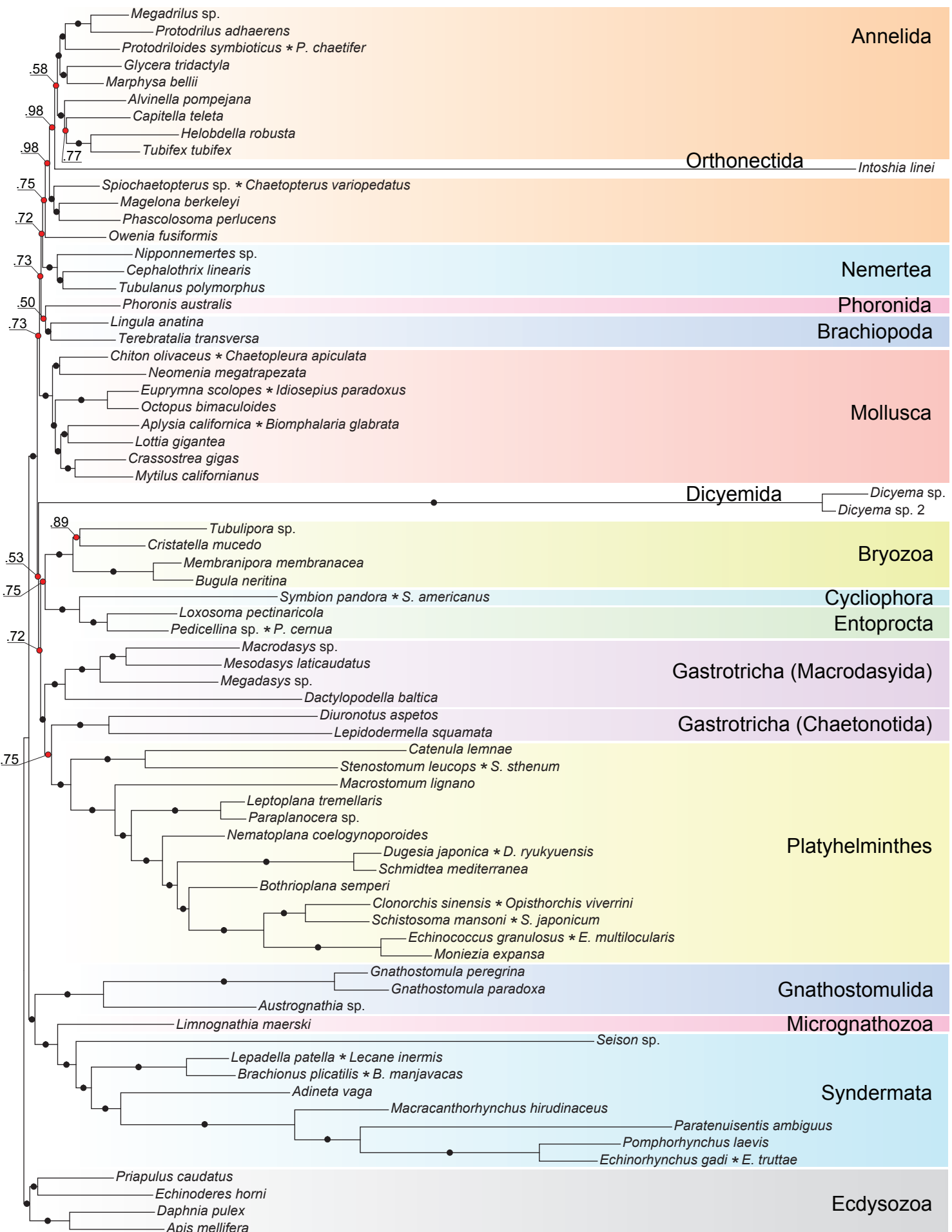
0.5



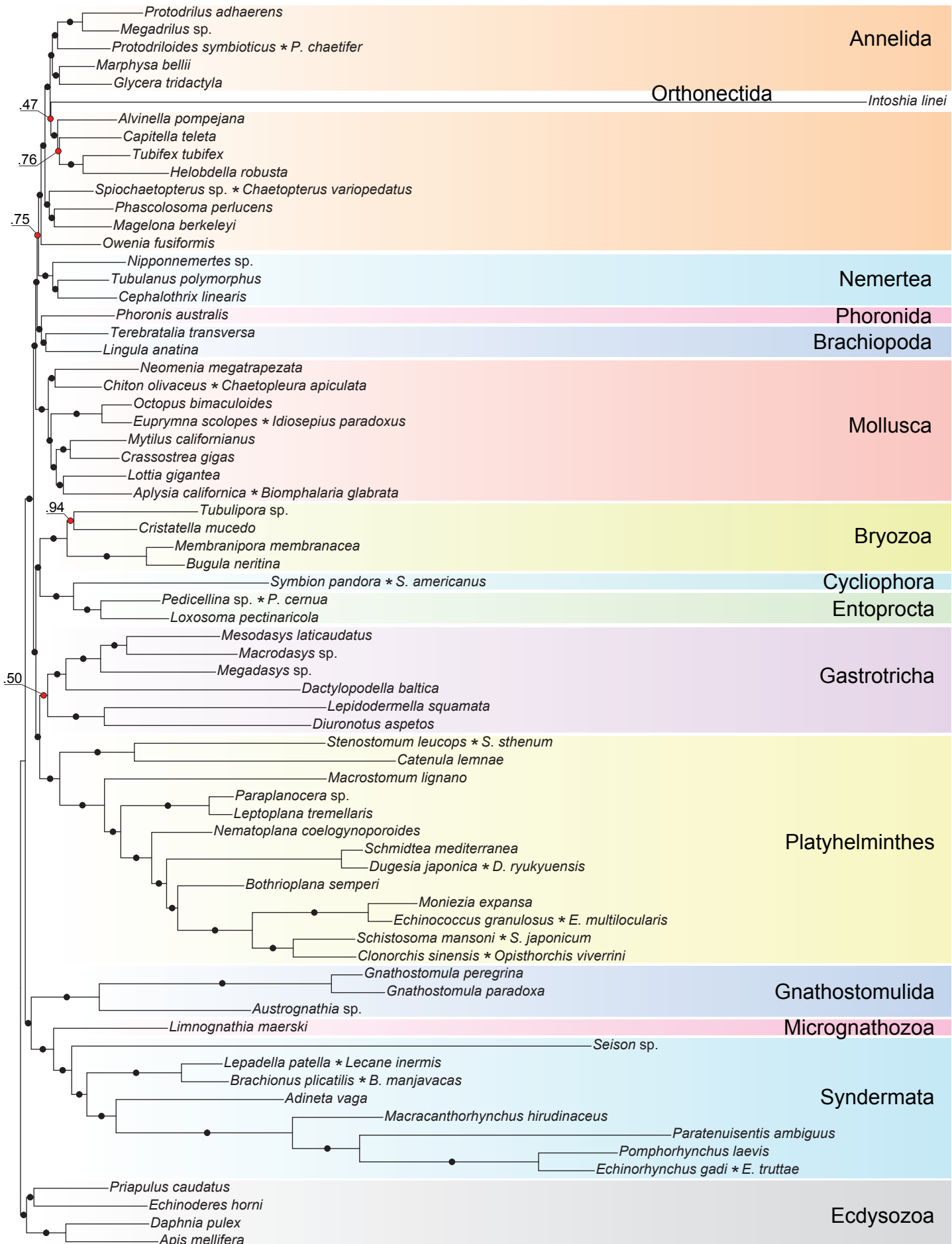
Supplementary Figure S4 (for page 13). Maximum likelihood reconstruction with RAxML. The tree was obtained under the PROTCATGTR model; support values are based on 150 rapid bootstrap replicates. Values of 100% are not shown, and corresponding nodes are marked with black dots. Chimeric operational taxonomic units include names of merged species signed with an asterisk.



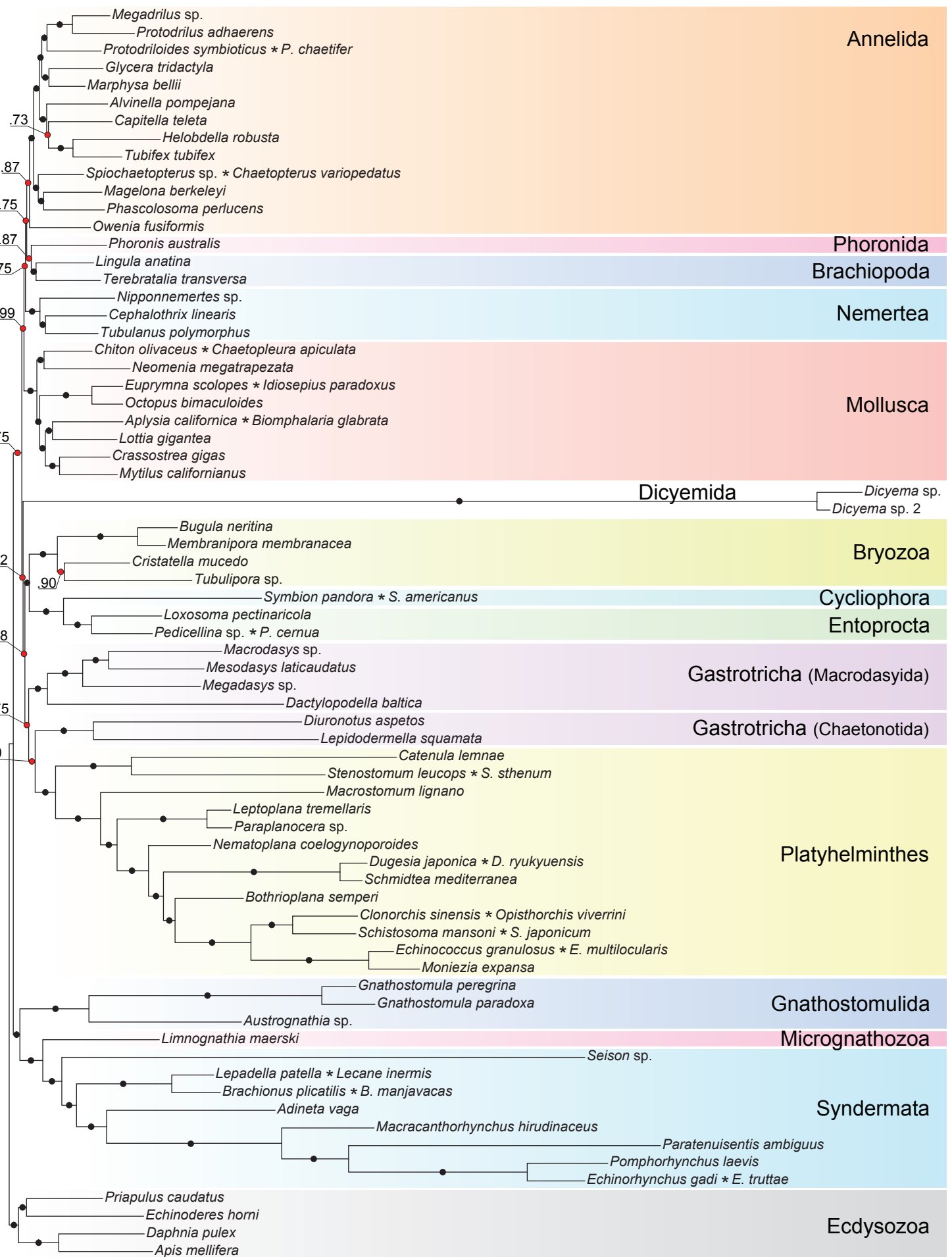
Supplementary Figure S5 (for page 13). Maximum likelihood reconstruction with IQ-TREE. The inference was performed under the LG+C60+F+G4 model; node support was evaluated with ultrafast bootstrap approximation (1000 replicates). Nodes with 100% support marked with black dots.



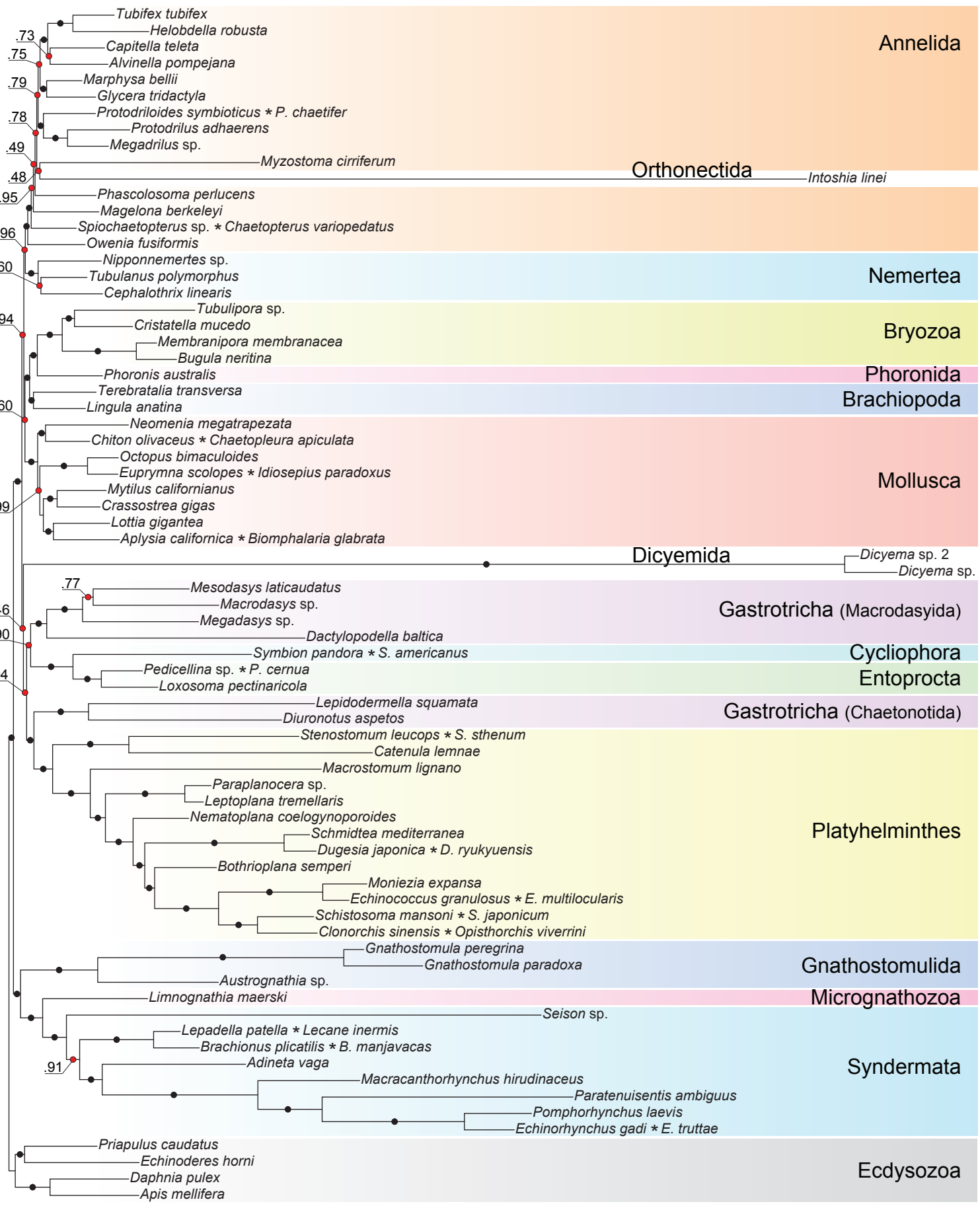
Supplementary Figure S6 (for page 14). Bayesian inference with the dataset excluding the annelid *Myzostoma cirriferum*. PhyloBayes was run with four chains under the CAT+GTR +Γ4 model. The consensus tree was constructed after 15,000 cycles with 50% burn-in (*maxdiff*=1.0). Only posterior probability values below 1.0 are shown.



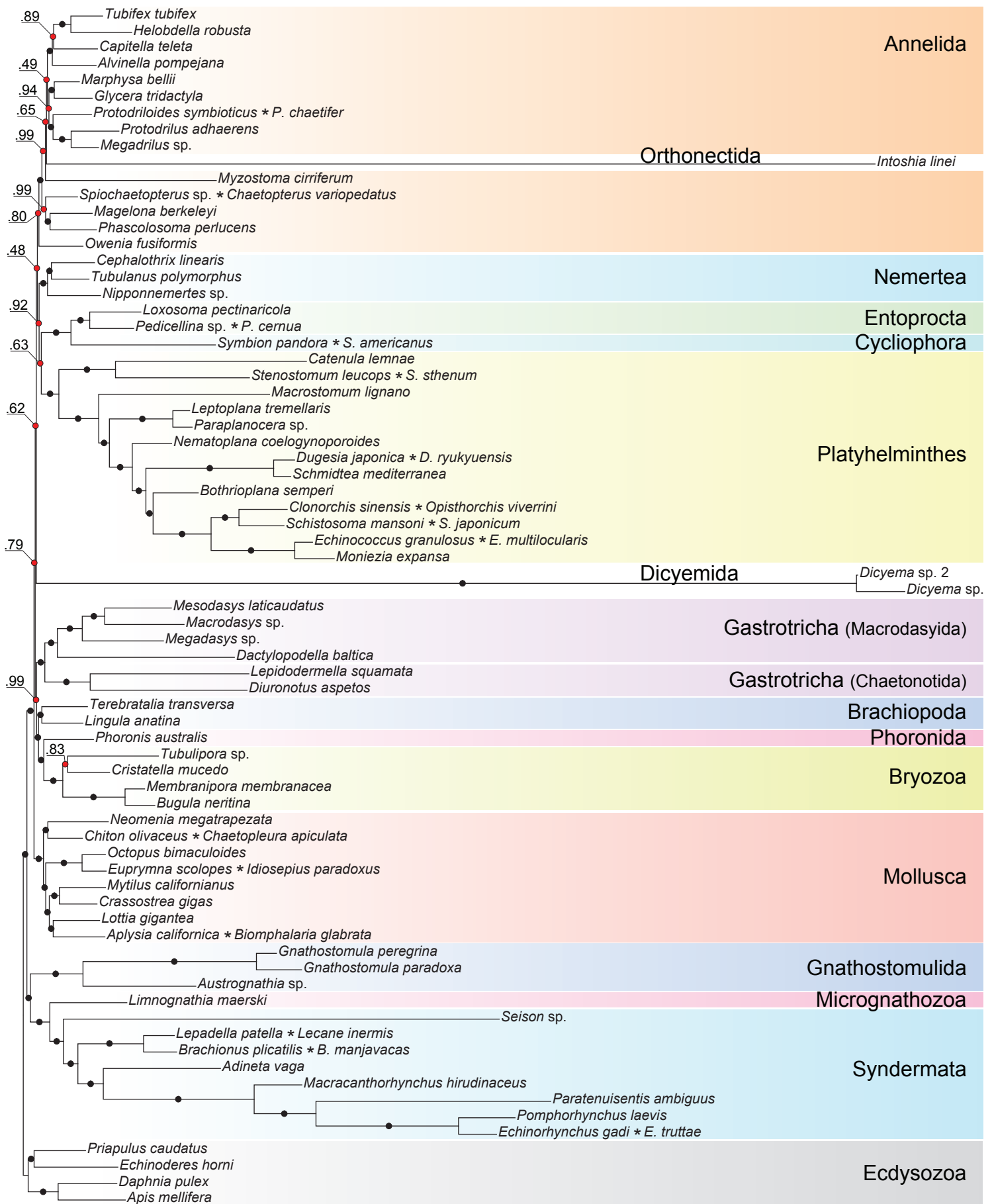
Supplementary Figure S7 (for page 14). Bayesian tree with the exclusion of two dicyemids and the annelid *Myzostoma cirriferum*. PhyloBayes was run with four chains under the CAT +GTR+Γ4 model. The consensus tree was constructed after 5,000 cycles with 50% burn-in (*maxdiff*=1.0). Only posterior probability values below 1.0 are shown.



Supplementary Figure S8 (for page 14). Bayesian tree with the exclusion of the orthonectid *Intoschia linei* and the annelid *Myzostoma cirriferum*. PhyloBayes was run with four chains under the CAT+GTR+G4 model. The consensus tree was constructed after 5,000 cycles with 50% burn-in (*maxdiff*=1.0). Only posterior probability values below 1.0 are shown.



Supplementary Figure S9 (for page 14). Bayesian inference with the 35K-site dataset excluding protein alignments with high compositional heterogeneity. The inference was carried out under the CAT+GTR+G4 model, and the tree was generated after 50,000 cycles with 50% burn-in (*maxdiff*=0.95).



Supplementary Figure S10 (for page 14). Bayesian inference with the Dayhoff-recoded alignment. The inference was carried out under the CAT+GTR+Γ4 model; the tree was generated after 30,000 cycles with 50% burn-in (*maxdiff*=0.17).